

# Silicon waveguide based TE mode converter

Jing Zhang,\* Tsung-Yang Liow, Mingbin Yu, Guo-Qiang Lo, and Dim-Lee Kwong

*Institute of Microelectronics, A\*STAR (Agency for Science, Technology and Research) 11 Science Park Road, Singapore Science Park II, Singapore 117685. Tel: (65) 67705391, Fax: (65) 67731914, Singapore*

*\*zhangj@ime.a-star.edu.sg*

**Abstract** A silicon waveguide based TE mode converter was designed for the mode conversion between a horizontal waveguide and vertical waveguide in the two-layer structure waveguide based polarization diversity circuit. The TE mode converter's performance was studied. The polarization mode converter with minimum length of  $5\mu\text{m}$  was demonstrated to provide the TE mode conversion while maintaining the polarization status. The insertion loss at the transition region was less than 2dB.

©2010 Optical Society of America

**OCIS codes:** (260.5430) Polarization; (250.5300) Photonic integrated circuits.

---

## References and links

1. M. A. Popović, T. Barwicz, M. S. Dahlem, F. Gan, C. W. Holzwarth, P. T. Rakich, M. R. Watts, H. I. Smith, F. X. Kärtner and E. P. Ippen, "Hitless-reconfigurable and bandwidth-scalable silicon photonic circuits for telecom and interconnect applications," Proceeding of OFC/NFOEC, 1 – 3 (2008).
2. Y. A. Vlasov, F. Xia, S. Assefa, W. M. J. Green, "Silicon micro-resonators for on-chip optical networks," Proceeding of CLEO/QELS, 1 – 2 (2008).
3. S. Nakamura, C. Tao, M. Ishizaka, M. Tokushima, Y. Urino, M. Sakauchi, I. Nishioka, K. Fukuchi, "Ultra-small one-chip color-less multiplexer/ demultiplexer using silicon photonic circuit," Proceeding of ECOC, 175 – 176 (2008).
4. H. Fukuda, K. Yamada, T. Tsuchizawa, T. Watanabe, H. Shinjima, and S. Itabashi, "Ultrasmall polarization splitter based on silicon wire waveguides," Opt. Express **14**(25), 12401–12408 (2006).
5. H. Fukuda, K. Yamada, T. Tsuchizawa, T. Watanabe, H. Shinjima, and S. Itabashi, "Polarization rotator based on silicon wire waveguides," Opt. Express **16**(4), 2628–2635 (2008).
6. H. Fukuda, K. Yamada, T. Tsuchizawa, T. Watanabe, H. Shinjima, and S. Itabashi, "Silicon photonic circuit with polarization diversity," Opt. Express **16**(7), 4872–4880 (2008).
7. M. R. Watts, H. A. Haus, and E. P. Ippen, "Integrated mode-evolution-based polarization splitter," Opt. Lett. **30**(9), 967–969 (2005).
8. M. R. Watts, and H. A. Haus, "Integrated mode-evolution-based polarization rotators," Opt. Lett. **30**(2), 138–140 (2005).
9. M. R. Watts, M. Qi, T. Barwicz, L. Socci, P. T. Rakich, E. P. Ippen, H. I. Smith, and H. A. Haus, "Towards integrated polarization diversity: design, fabrication, and characterization of integrated polarization splitters and rotators," 2005 Optical Fiber Communications Conference Postdeadline Papers, **5**, (2005).
10. T. Barwicz, M. R. Watts, M. A. Popović, P. T. Rakich, L. Socci, F. X. Kärtner, E. P. Ippen, and H. I. Smith, "Polarization-transparent microphotonic devices in the strong confinement limit," Nat. Photonics **1**(1), 57–60 (2007).
11. M. Romagnoli, L. Socci, L. Bolla, S. Ghidini, P. Galli, C. Rampinini, G. Mutinati, A. Nottola, A. Cabas, S. Doneda, M. Di Muri, R. Morson, T. Tomasi, G. Zuliani, S. Lorenzotti, D. Chacon, S. Marinoni, R. Corsini, F. Giacometti, S. Sardo, M. Gentili, and G. Grasso, "Silicon Photonics in Pirelli," in Silicon Photonics and Photonic Integrated Circuits. Edited by Righini, Giancarlo C.; Honkanen, Seppo K.; Pavesi, Lorenzo; Vivien, Laurent. Proceedings of the SPIE, **6996**(699611), 1–8 (2008).
12. J. Zhang, M. Yu, G. Lo, and D. L. Kwong, "Silicon waveguide based mode-evolution polarization rotator," IEEE J. Sel. Top. Quantum Electron. **16**(1), 53–60 (2010).
13. V. R. Almeida, R. R. Panepucci, and M. Lipson, "Nanotaper for compact mode conversion," Opt. Lett. **28**(15), 1302–1304 (2003).

---

## 1. Introduction

Silicon photonics received much attention in the recent years. Silicon waveguides have great potential as a platform for ultra-small photonic circuits [1–3]. Modulators, photo-detectors, filters, switches, waveguides based on silicon wire have been demonstrated. However, silicon waveguide has large structural birefringence which causes polarization mode dispersion,

polarization dependent loss, and polarization dependent wavelength characteristics. The polarization mode dispersion will affect devices application in high data rates. The difference in the effective polarization modes indices makes the filters' resonance wavelengths different. The polarization dependent characteristics limit the application of silicon photonics devices.

To make a photonic circuit polarization independent, one common way is to implement polarization diversity scheme. The light with arbitrary polarization from the source will be split into orthogonal component by polarization splitter. By further rotating one of the components, a single polarization is achieved. The two paths may be operated in parallel with identical structures. The polarization splitters, rotators, and the functional devices can be integrated on the same chip.

Fukuda et al. in NTT designed and fabricated mode-coupling-based polarization splitters [4] and rotators [5] in silicon waveguides. A 35  $\mu\text{m}$  long polarization rotator with polarization extinction ratio (PER) of 11dB was demonstrated based on an off-axis double-core structure consisting of a silicon waveguide and SiOxNy waveguide. Fukuda et al. applied their polarization splitter and rotator in a wavelength filter and achieved improvement for 10Gbps data transmission [6]. The mode-coupling-based rotator has the advantage of single layer of silicon waveguide, but it has very small dimensional tolerance in fabrication. However, the mode-evolution-based rotator has better 90 degree rotation effect with larger wavelength operation window. Watts et al. in MIT first published were silicon nitride based mode-evolution-based polarization splitters [7] and rotators [8]. The waveguides had core indices of 2.2 and dimensions of 800nm(w)  $\times$  400nm(h) (horizontal waveguide) for TE mode waveguide and 400nm(w)  $\times$  800nm(h) (vertical waveguide) for TM mode waveguide. The two-layer waveguide based polarization rotator was about 200 $\mu\text{m}$  long. A silicon nitride based integrated mode-evolution-based polarization splitter and rotator (PSR) was first reported in [9]. The best standalone polarization rotator exhibited -18dB cross-talk across the band. In 2006, a polarization-transparent add-drop filter was demonstrated with the mode-evolution-based polarization splitter-rotator (PSR) in silicon nitride waveguide [10]. In 2008, Romagnoli et al. in Pirelli demonstrated an integrated two-layer PSR in silicon channel waveguide with cross-section of 450nm  $\times$  220nm [11]. The polarization rotation efficiency improved monotonically with the increase of PSR length. The rotation efficiency was basically constant in C-band. The rotator conversion performance was achieved to be 13dB PER with 200 $\mu\text{m}$  PSR length and 20dB PER with 300 $\mu\text{m}$  PSR.

In [12], a further scaled down of mode-evolution-based polarization rotator in silicon waveguide was achieved. The rotator's performance was studied under different launching conditions. It was founded in the experiments that the rotator had better optical insertion loss and PER at the abnormal launching condition. The rotator with minimum length of 40 $\mu\text{m}$  was demonstrated to provide the polarization rotation with polarization extinction ratio of 15dB at the abnormal launching condition. The insertion loss at the transition region was less than 1dB. At the abnormal launching condition, the TM mode in the horizontal waveguide rotates to TE mode in the vertical waveguide.

To take the advantage of the silicon waveguide based polarization rotator at the abnormal launching condition, we propose a new PSR consisting of a mode-coupling-based polarization splitter [4] which splits the TE mode and the TM mode into two horizontal waveguides, a two-layer polarization rotator [12] which rotates the TM mode in horizontal waveguide to the TE mode in vertical waveguide, and a two-layer TE mode converter which converts the TE mode in vertical waveguide to the TE mode in horizontal waveguide. In this paper, we present the two-layer polarization mode converter. It is designed in 400nm  $\times$  200nm silicon waveguide. It converts the TE mode between 400nm (height)  $\times$  200nm (width) horizontal waveguide and 200nm (height)  $\times$  400nm (width) vertical waveguide. With the polarization rotator in [12] and the new polarization mode converter, TM mode in horizontal waveguide can be converted into TE mode in the same waveguide. The converter's performance is studied. Simulations and experimental results are presented.

## 2. Design of silicon waveguide based TE mode converter

The principle of the polarization mode converter is adiabatic mode size conversion. The polarization mode converter is in  $400\text{nm} \times 200\text{nm}$  silicon waveguide. It includes a pair of waveguide core layers. Low loss mode converter needs a transition region between the input and output. The transition region is designed to have symmetric lateral taper and pseudo-vertical taper shape. Figure 1 shows the core waveguide structure of the polarization mode converter. The cross-sections along the waveguide are shown in Fig. 2. The waveguide core is silicon with index of 3.5. The cladding is silicon dioxide with index of 1.45.

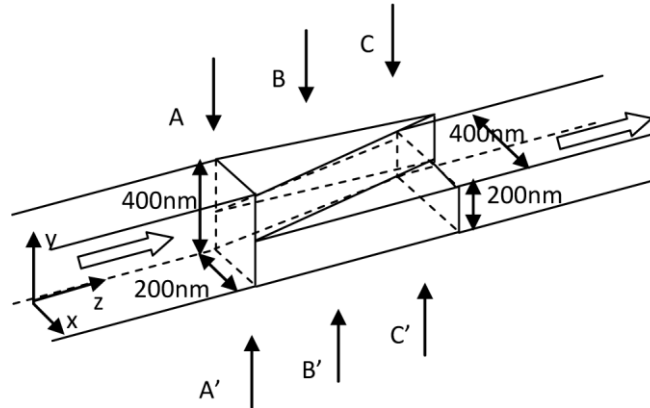


Fig. 1. The design of silicon waveguide based polarization mode converter.

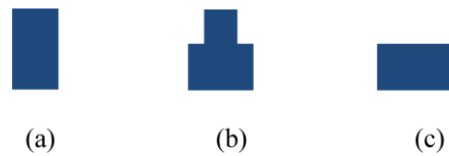


Fig. 2. Cross-sections of the waveguide at (a) A-A', (b) B-B', and (c) C-C' in transition region.

The length of the transition region will affect the optical insertion loss of the TE mode converter. When the transition region is too short, the mode mismatching between the horizontal and vertical waveguide will cause light leakage in the transition region. If the transition region is too long, the optical propagation loss will increase. The optical insertion loss of the TE mode converter was studied by using 3D FDTD simulation. The calculation length of the waveguide was  $30\mu\text{m}$ . Figure 3 shows the insertion loss of the TE mode converter across the transition length. The insertion loss increase rapidly when the transition length is less than  $5\mu\text{m}$ .

The length of the transition region was designed to be from  $5\mu\text{m}$  to  $30\mu\text{m}$ . We studied the performance of the polarization mode converter in  $400\text{nm} \times 200\text{nm}$  silicon waveguide when launching with TE mode. TE mode is transverse electrical field. Figure 4(a) shows the TE mode in  $200\text{nm}$  (w)  $\times$   $400\text{nm}$  (h) waveguide (vertical waveguide) at the input. Figure 4(g) shows the TE mode in  $400\text{nm}$  (w)  $\times$   $200\text{nm}$  (h) waveguide (horizontal waveguide) at the output. Three-dimensional finite-difference-time-domain (FDTD) simulations were performed with center wavelength at  $1550\text{nm}$ . The grid size was  $20\text{nm}$  in x-axis,  $20\text{nm}$  in y-axis, and  $40\text{nm}$  in z-axis.

To simulate the polarization mode conversion, continuous TE mode was launched at the input plane  $z = 0\mu\text{m}$  and both TM and TE modes were monitored along the transition region. In the transition region, TE mode profile gradually converts as the waveguide gradually transforms from a vertical waveguide ( $400\text{nm}$  height  $\times$   $200\text{nm}$  width) to a horizontal

waveguide (200nm height  $\times$  400nm width). Figure 4(a)–4(g) show the TE mode profiles in the transition region from the input to the output.

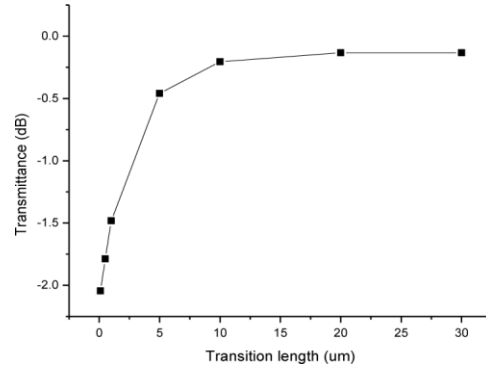


Fig. 3. The insertion loss of the TE mode converter across the transition length.

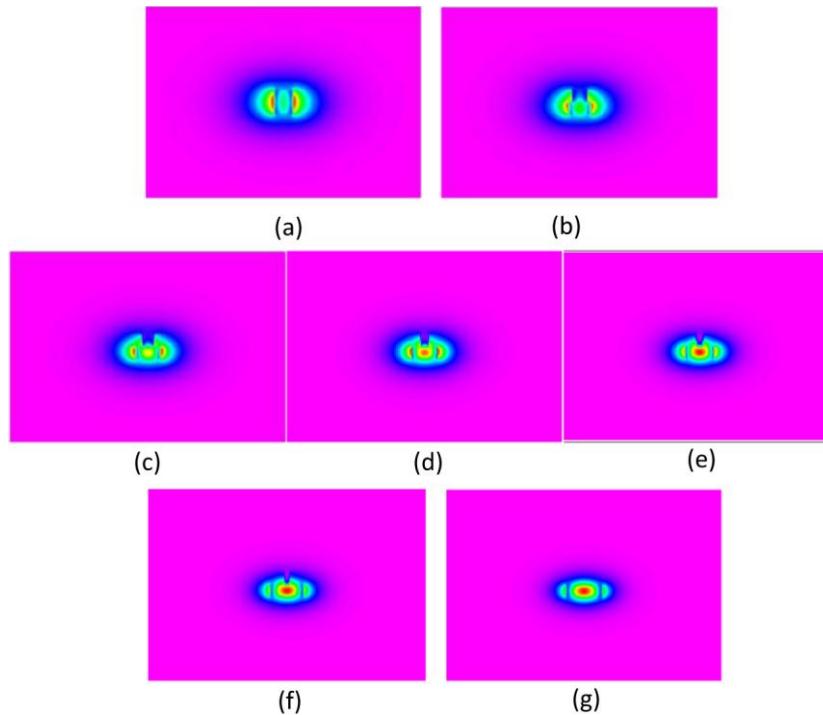


Fig. 4. (a)-(g) TE mode profiles in transition waveguide from the input to the output.

Figure 5 shows the  $E_x$  waves propagation along a 30 $\mu\text{m}$  polarization mode converter.  $E_x$  is the electrical field component in x-axis. In the 3D FDTD simulations, the majority of the field of TE mode is  $E_x$ . At the output, the average amplitude of  $E_x$  and  $E_y$  were monitored by using a monitor in simulation. Figure 6 shows the time response of the monitor placed at the output. The average  $E_y$  field is 0. Hence the simulation shows that the polarization mode converter can convert the mode while maintaining the polarization status.

The polarization mode converter's wavelength dependence was studied with FDTD simulation in a 10 $\mu\text{m}$  length device under pulse incidence condition. The center wavelength in the simulation was 1550nm. It was found that the polarization mode converter has flat response across the wavelength.

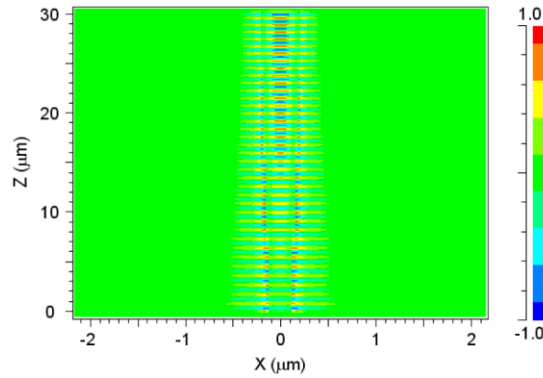


Fig. 5. Ex component propagation along the polarization mode converter.

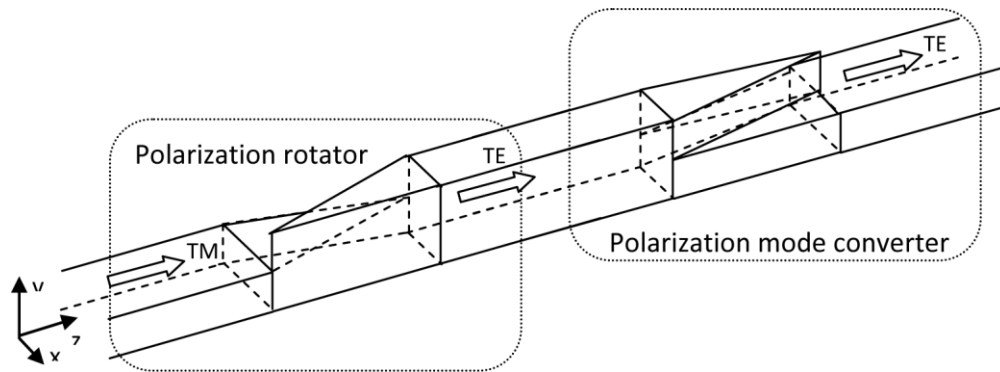


Fig. 6. Combined polarization rotator and mode converter.

By combining the polarization rotator in [12] with the proposed polarization mode converter (Fig. 6), a polarization rotation from TE to TM or from TM to TE between horizontal waveguides will be realized.

### 3. Fabrication and experiments

The polarization mode converter waveguides were fabricated on SOI wafer. The bottom oxide layer (BOX SiO<sub>2</sub>) was 2 μm thick. The top silicon was 400 nm thick. The two-layer waveguide structure was processed by two-step dry etching. The waveguide outline (the first layer) was fabricated by reactive ion etching silicon 400 nm to buried oxide layer. The taper was patterned by a second layer lithography and partial etched 200 nm. The critical dimension of the tip size in the mask is 180 nm. By tuning the exposure energy in lithography process, the tip size was achieved to be around 100 nm at the tip. 2 μm top SiO<sub>2</sub> cladding layer was deposited by High Density Plasma PECVD (HDP SiO<sub>2</sub>) in Applied Material PECVD chamber.

Devices with different length were fabricated to accommodate the fabrication uncertainties. The transition lengths of the TE converters were from 5 μm to 30 μm. The total waveguide length was 3 mm. The waveguide was tapered to 180 nm width at the both ends. The waveguide was 200 nm (w) and 400 nm (h) and it started to transit to 400 nm (w) and 200 nm (h). Figure 7 shows the SEM picture of the transition region of the two-layer TE mode converter.

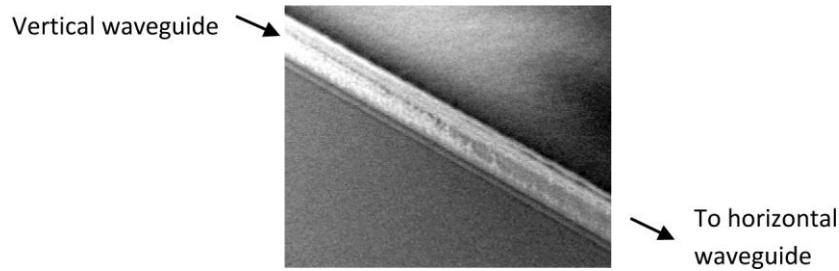


Fig. 7. SEM picture of the two-layer structure at the transition region of polarization mode converter.

A broadband ASE source was used to characterize the devices. It covered the wavelength range from 1530nm to 1570nm. Polarization maintenance fibers were used in connection. The light source was polarized with a polarizer. The output power after the polarizer was  $-1\text{dBm}$ . By changing the angle of the polarizer, the polarization status of the light could be changed. The power fluctuation caused by changing the polarization status was less than  $0.1\text{dB}$ . At the output, another polarizer was connected in the measurement system to check the light polarization status at the output. With the second polarizer, the total output optical power was  $-6\text{dBm}$ . The polarization extinction ratio of the light source with polarization controller was more than  $20\text{dB}$ . We measured a simple silicon waveguide on this wafer and the propagation loss in a  $3\text{mm}$  long horizontal waveguide plus the coupling loss between the lensed fiber and the waveguide was estimated to be about  $5.5\text{dB}$  with the setup. We measured the insertion loss and PER of the TE polarization mode converter at two launching directions. In the experiment, the optical coupling between the lensed-fiber and waveguide in the experiment had almost  $\pm 0.5\text{dB}$  variation due to loading and unloading.

### 3.1 Launching TE mode from in $200\text{nm}$ ( $w$ ) and $400\text{nm}$ ( $h$ ) waveguide and getting output in $400\text{nm}$ ( $w$ ) and $200\text{nm}$ ( $h$ ) waveguide

**Table 1. Insertion losses and polarization extinction ratios of the TE mode converter**

Transition length ( $\mu\text{m}$ )	Insertion loss at transition region (dB)	PER (dB)
5	1.1	17.0
10	1.2	17.2
30	1.2	16.9

In this measurement,  $-1\text{dBm}$  light in TE mode was launched into the vertical waveguide with dimensions of  $200\text{nm}$  ( $w$ ) and  $400\text{nm}$  ( $h$ ). TE mode converters with transition length of  $5\mu\text{m}$ ,  $10\mu\text{m}$ , and  $30\mu\text{m}$  were tested with the second polarizer at the output. The light output power was measured to be around  $-12.6\text{dBm}$ . Considering the  $5.5\text{dB}$  coupling loss and propagation loss from the silicon waveguide, and another  $5\text{dB}$  loss from the second polarizer, the TE mode converter transition region contributed  $1\text{dB}$  loss in TE mode conversion. The polarization extinction ratio at the output was around  $17\text{dB}$ . The measurement results are listed in Table 1.

### 3.2 Launching TE mode from in $400\text{nm}$ ( $w$ ) and $200\text{nm}$ ( $h$ ) waveguide and getting output in $200\text{nm}$ ( $w$ ) and $400\text{nm}$ ( $h$ ) waveguide

**Table 2. Insertion losses and polarization extinction ratios of the TE mode converter**

Transition length ( $\mu\text{m}$ )	Insertion loss at transition region (dB)	PER (dB)
5	1.9	17.1
10	1.9	17.3
30	2.1	16.9

In this measurement, light in TE mode was launched to the horizontal waveguide with dimensions of  $400\text{nm}$  ( $w$ ) and  $200\text{nm}$  ( $h$ ). TE mode converters with transition length of  $5\mu\text{m}$ ,

10 $\mu$ m, and 30 $\mu$ m were tested. The light output power was measured to be around -13.4dBm with -1dBm input power. Considering the 5.5dB coupling loss and propagation loss, the TE mode converter transition region contributed 2 dB loss in TE mode conversion. The polarization extinction ration at the output was around 17dB. The experiment also shows the converter has a flat response in the range from 1530nm to 1570nm. The measurement results are listed in Table 2.

For a passive optical component, 1 to 2dB insertion loss is not small enough. The coupling loss plus the propagation loss is 5.5dB. The total loss of a TE mode converter in a 3mm long waveguide is 6.5 to 7.5dB. To reduce the propagation loss, the side walls and the partial etched surface of the waveguide need to be smooth in fabrication. The surface roughness will also affect the insertion loss of at the transition region. The surface roughness can be reduced by silicon thermal oxidation process. The coupling between the silicon waveguide and the lensed-fiber can be improved by further narrowing silicon waveguide tip size [13]. In this fabrication, the waveguide tip size at the coupling facet is about 180nm width. If it is further narrowed down to about 120nm width, the coupling efficiency can be improved to 0.5dB per coupling theoretically [13].

#### **4. Conclusions**

High efficient wideband silicon waveguide based TE mode converters were demonstrated in 400nm  $\times$  200nm silicon waveguide. Simulations and experiments were carried. The mode conversions are constant for the converters with transition lengths from 5 $\mu$ m to 30 $\mu$ m. Less than 2dB loss at the transition region, and more than 17dB extinction ratio were achieved in the polarization mode conversion between the TE mode in 200nm (w) and 400nm (h) waveguide and TE mode in 400nm (w) and 200nm (h) waveguide. By cascading the proposed polarization mode converter with the polarization rotator in [12], the polarization rotation can be achieved between two identical horizontal silicon waveguides. Hence, a new PSR consisting of a mode-coupling-based polarization splitter as in [4], a two-layer polarization rotator as in [12], and a two-layer TE mode converter will be enabled.

#### **Acknowledgement**

This work was supported by the Science and Engineering Research Council of A\*STAR (Agency for Science, Technology and Research), Singapore. The SERC grant number: 0921150116.